Journal of The Electrochemical Society, **158** (5) D254-D258 (2011)
0013-4651/2011/158(5)/D254/5/$28.00 © The Electrochemical Society

Removal of Anodic Aluminum Oxide Barrier Layer on Silicon Substrate by using Cl_2/BCl_3 Neutral Beam Etching

J. K. Yeon,[a] W. S. Lim,[b] J. B. Park,[b] N. Y. Kwon,[b] S. I. Kim,[c] K. S. Min,[a] I. S. Chung,[b] Y. W. Kim,[c] and G. Y. Yeom[a,b,z]

[a]*Department of Advanced Materials Science and Engineering, Sungkyunkwan University, Suwon, Korea*
[b]*Sungkyunkwan Advanced Institute of Nanotechnology, Suwon, Korea*
[c]*Department of Materials Science and Engineering, Seoul National University, Sillim 9-dong Gwanak-gu, Seoul, Korea*

The barrier layer of anodic aluminum oxide (AAO) formed on the silicon substrate was etched with Cl_2/BCl_3 gas mixtures by a neutral beam and the results were compared with the AAO etched by an ion beam. The etch rate of AAO itself was increased with the increase of BCl_3 in Cl_2/BCl_3 up to 60% in the gas mixture. And, the etching of AAO itself was related to the Cl radical density in the plasma and the formation of volatile BO_xCl_y on the AAO surface for both the neutral beam etching and the ion beam etching. The AAO itself could be etched by both the neutral beam and the ion beam in all Cl_2/BCl_3 gas mixtures. However, the barrier layer of the AAO located near the bottom of the AAO pore could not be etched using the ion beam etching due to the charging of the nanometer size AAO pore similar to the case of conventional reactive ion etching. Using the neutral beam etching, the barrier layer of AAO pore could be successfully etched with BCl_3-rich BCl_3/Cl_2 gas mixtures by removing the barrier layer without charging the AAO pore and by the forming volatile BO_xCl_y.
 [DOI: 10.1149/1.3561421]

Manuscript submitted December 9, 2010; revised manuscript received February 7, 2011. Published March 17, 2011.

Anodization is a technology transforming metal into metal oxide by electrochemical oxidation and it has been actively investigated for the fabrication of nanostructure of various sizes. Especially, the anodic aluminum oxide (AAO) obtained by the anodization of aluminum film is being used as the template and mask for deposition, etching, doping, etc. in the fabrication of various nano devices such as magnetic data storage devices, optoelectronic devices, nano sensors, etc.[1–4]

In general, AAO can be fabricated with various porous nano-hole spacing and diameter in the range of 10–500 and 4–200 nm by controlling anodization voltage and, also by using indentation method, various shapes of AAO such as hexagonal, square, and triangular shaped AAO can be fabricated.[5–7] When the AAO is used as the solid mask, due to the strong bonding of Al_2O_3, it shows superior mechanical properties compared to other porous mask materials.[8] Especially, compared to the patterning using electron-beam lithography and block co-polymer, the patterning using AAO is cheaper, more reliable, and easier in controlling the size and shape.[9] In addition, it can be applied to fabricate various two-dimensional lateral superlattice structures by using highly ordered AAO templates.[10] However, due to the stress at the interface between the aluminum and the substrate, the alumina barrier layer is formed at the bottom of the AAO holes during the formation of AAO and it prevents direct physical and electrical contact to the substrate, and it is known to be one of the biggest problems in the formation of AAO.[11,12]

To remove the barrier layer, various techniques such as pore widening, cathodic polarization, voltage drop, plasma assisted etching, etc. are investigated.[13–15] In the case of pore widening and cathodic polarization, even though the barrier layer can be removed reliably and reproducibily, due to the chemical attack of the sidewall of AAO by OH- formed during the removal of the barrier layer, the AAO pore diameter is increased. Therefore, it is difficult to have AAO having less than 50 nm diameter after the removal of the barrier layer. In the case of voltage drop method, where the anodization voltage is decreased during the last period of the anodization, even though the thickness of the barrier layer can be decreased during the formation of the AAO, it is difficult to remove permanently in addition to the lack of reproducibility. The removal of the barrier layer was investigated by using plasma assisted etching such as reactive ion etching to remove the barrier layer without widening the AAO pore diameter, however, possibly due to the change of ion beam trajectory by the surface charging effect, it was difficult to remove the barrier layer located at the bottom of AAO pore.[16]

[z] E-mail: gyyeom@skku.edu

Previously, a neutral beam etching has been investigated to etch the materials without surface charging by using a highly directional radical beam instead of conventional reactive ions by the plasma assisted etching.[17] In this study, to remove the barrier layer of AAO more effectively without widening of the AAO pore diameter, the Cl_2/BCl_3 neutral beam etching has been used and the effect of neutral beam on the removal of the barrier layer has been investigated. To study the effect of surface charging on the removal of the barrier layer during the AAO etching, the AAO was also etched with Cl_2/BCl_3 ion beams and the etch characteristics were compared.

Experimental

AAO was fabricated by evaporating about 2 μm thick aluminum thin film on p-type Si (100) wafers using an e-beam evaporator followed by two-step anodization. The first step anodization was carried out in 0.3 M oxalic acid using 40 V at 4°C for about 76 min and the aluminum oxide formed during the first anodization was removed in a solution composed of 1.8 wt % H_2CrO_4 and 7.4 wt % H_3PO_4 at 65°C for 2 h. The second step anodization was carried out in the same condition as the first anodization for 300 s. The AAO pore diameter and depth formed after the second step anodization were 36.7 ± 2.3 and 215.3 ± 5.7 nm, respectively, and the barrier thickness was 15 ± 1.9 nm. To remove the surface roughness in the AAO pore after the anodization, the AAO was treated in 5.0 wt % H_3PO_4 solution for 5 min at room temperature.

The neutral beam etching equipment used in this experiment was composed of a three-grid-type inductively coupled plasma (ICP) ion gun for the generation of reactive ion beam and a reflector for the neutralization of the reactive ions. The ICP ion gun was operated using 13.56 MHz rf power and the energy of the ion beam was controlled by the first grid voltage while the flux and directionality of the ion beam was controlled by the second grid. The third grid was grounded. A parallel reflector plates tilted 5° to the ion beam were installed in front of the third grid for the neutralization of the ion beam through the low angle reflection of the ion beam on the reflector plate. The grids and the reflector plates were made of graphite. To operate the system as the ion beam system instead of the neutral beam system, the reflector plates installed in front of the grids were removed. The details of the neutral beam etching system can be found elsewhere.[18]

The AAO samples were etched at room temperature using Cl_2/BCl_3 gas mixtures. The etch depth and the etch shape of the AAO were observed using a field emission scanning electron microscope (FESEM, Hitachi, S-4700). The etched shapes of AAO were

also observed by cross-sectional transmission electron microscopy (TEM, JEOL 2010F). The residue state of the AAO pore was analyzed using the micro energy dispersive X-ray spectroscopy (EDX) installed in TEM. The chemical states of the etched AAO surface was also investigated using angular resolved x-ray photoelectron spectroscopy (XPS, Thermo VG, MultiLab 2000, Mg Kα source). The plasma characteristics of Cl_2 / BCl_3 gas mixture were observed using optical emission spectroscopy (OES, Avaspec-3648).

Results and Discussion

The AAO samples were etched using the neutral beam and the ion beam with Cl_2/BCl_3 gas mixture and the etch rates are shown in Fig. 1 as a function of gas mixing ratio. The total gas flow rate was maintained at 10 sccm while keeping the first grid voltage at 500 V, the second grid at −700 V, and the ICP power at 300 W. The etch rate was estimated by measuring the decreased height of the AAO thickness after the etching. As shown in Fig. 1, the increase of BCl_3 up to 60% increased the AAO etch rate from 55 to 98.5 Å/min for the neutral beam and from 86 to 225.2 Å/min for the ion beam. However, the further increase of BCl_3 to 100% decreased the etch rate for both the neutral beam and the ion beam to 77.5 and 191 Å/min, respectively. Therefore, the ion beam showed higher etch rate than the neutral beam. The decrease of etch rate for the neutral beam was more related to the lower physical bombardment effect caused by the decreased beam flux due to the scattering and the decreased energy of the beam during the reflection of the ion beam on the reflector plate at the same etch conditions.[19]

The plasma characteristics of the ICP source used for the neutral beam and the ion beam were measured using OES and the optical emission intensities of B, BCl, and Cl located at 249.4, 272, and 774.5 nm, respectively, were measured as a function of Cl_2/BCl_3 gas mixture and the results are shown in Fig. 2. (The optical emission intensity is proportional to not only the radical density but also the electron density. When BCl_3 is mixed with Cl_2 while keeping same rf power and same pressure, no significant change of electron density is expected. Therefore, we used the optical emission intensity in Fig. 2 as the estimation of radical density.) The plasma condition was kept same as the condition in Fig. 1. As shown in Fig. 2, the optical emission peaks such as B and BCl were increased with the increase of BCl_3 percentage due to the increase of BCl_3 in the gas mixture. In the case of Cl OES peak, the increase of BCl_3 percentage in the gas mixture up to 60% also increased the Cl emission intensity. However, the further increase of BCl_3 to 100% decreased the Cl atomic optical emission intensity possibly indicating the highest Cl atomic density at 60% BCl_3. The initial increase of Cl atomic optical emission intensity in the plasma with the increase of BCl_3 is believed to be related to the increased dissociation of BCl_3 which contains more Cl atoms than Cl_2. On the other hand, when the BCl_3 percentage is increased higher than 60%, the Cl radical density in the plasma was decreased possibly due to the decreased dissociation of BCl_3 and the increased condensation of BCl_3 on the ICP source chamber wall with the increase of BCl_3 percentage in Cl_2/BCl_3 gas mixture which decreases the total Cl atomic density available in the ICP source. The similarity of Cl atomic optical emission intensity measured as a function of Cl_2/BCl_3 gas mixture in Fig. 2 with the etch rates by the neutral beam and the ion beam measured as a function of Cl_2/BCl_3 in Fig. 1 indicates the etch rate of AAO is partially related to the Cl atomic flux (and Cl^+ ion flux) to the AAO surface as studied by other researcher.[20]

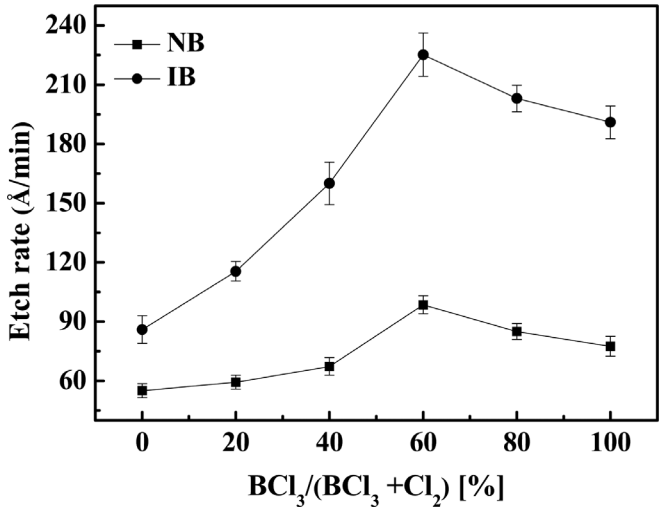

Figure 1. Etch rate of AAO (anodic aluminum oxide) for a neutral beam etching and an ion beam etching as a function of Cl_2 / BCl_3 gas mixing ratio.

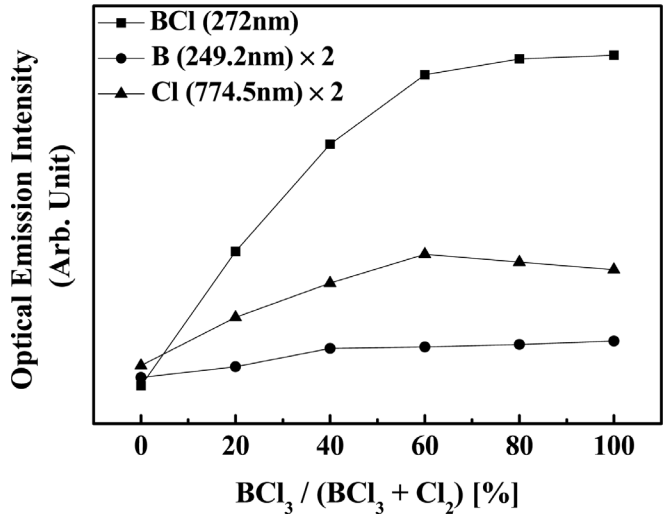

Figure 2. OES intensity of Cl radical as a function of Cl_2 / BCl_3 gas mixing ratio for the etching conditions in Fig. 1.

AAO samples were etched by the neutral beam and Fig. 3 shows the FESEM micrographs of (a) AAO before etching, (b) AAO after the etching by pure Cl_2, and (c) AAO after the etching by pure BCl_3. The AAO samples in (b) and (c) were etched with the total gas flow of 10 sccm while keeping the first grid voltage at 500 V, the second grid at −700 V, and the ICP power of the ion gun at 300 W. The etching was carried out for about 8–9 min. Figure 3a shows the barrier layer of AAO with the thickness of 15 nm before the etching which is caused by the stress pushing upward at the interface of silicon and AAO pore during the anodization.[21] As shown in Figs. 3b and 3c, when AAO was etched using pure Cl_2, the barrier layer was not easily removed even though the AAO top layer was significantly etched and the size of the AAO pore appeared to be decreased by blocking the sidewall of the hole with an etch residue. However, when AAO was etched using pure BCl_3, the barrier layer was easily removed and no significant change in the size of AAO pore was observed.

Figure 4 shows cross-sectional TEM micrographs of AAO after the etching by pure Cl_2 neutral beam. As shown in the TEM micrographs, a residue blocking the AAO pore near the top side of the AAO (shown as a circle) could be clearly observed. The top residue layer for the AAO etched using pure Cl_2 was analyzed using a micro EDX and its result is compared with the surface of the AAO etched by pure BCl_3 and the results are shown in Fig. 5. As shown in Fig. 5, the residue showed higher oxygen and chlorine compared to the surface etched by pure BCl_3. Therefore, less volatile $AlCl_xO_y$ residue appears to be formed during the etching and re-deposited on the sidewall and bottom of the AAO pore and, finally, the AAO pore was blocked by the less volatile compound. In fact, in the etching of aluminum oxide, the free energy change of the reaction ($Al_2O_3 + Cl_2 \rightarrow AlCl_x + O_2$) is positive, therefore, the etching of alumina by pure Cl_2 is not caused by a spontaneous reaction. However, the reaction of

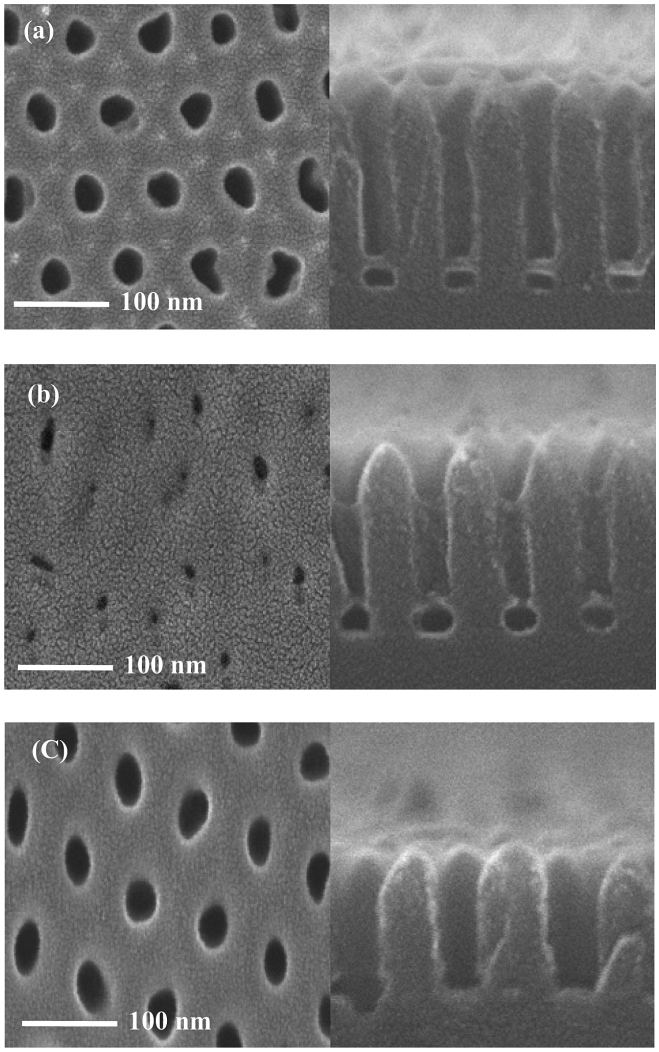

Figure 3. SEM micrographs of AAOs on silicon (a) before etching, (b) after the etching with pure Cl_2, and (c) after the etching with pure BCl_3 using the neutral beam etching.

$Al_2O_3 + BCl_3 \rightarrow AlCl_x + BO_xCl_y$ is thermodynamically feasible. That is, Al_2O_3 is more easily etched by BCl_3 not by Cl_2 even though the ion bombardment increases the chemical reactivity of Al in Al_2O_3 with Cl_2. Therefore, the easier etching of the barrier layer by BCl_3 compared to Cl_2 is related to the spontaneous formation of volatile BO_xCl_y during the etching.

Table I shows the atomic percentage of AAO surface before and after the etching by the neutral beam using Cl_2/BCl_3 gas mixtures. The other etching conditions are the same as those in Fig. 3. As shown in the table, after the etching by Cl_2, the oxygen percentage was increased from 73.3 to 76.5% in addition to the detection of 2.7% chlorine. By increasing the BCl_3 percentage to 100%, the oxygen percentage and chlorine percentage were decreased to 70.8 and 0.5%, respectively. The increase of oxygen percentage by the etching of pure chlorine is similar to micro EDX shown in Fig. 5 and is related to the difficulty of oxygen removal from the AAO by pure chlorine and the formation of less volatile $AlCl_xO_y$ as the residue. However, as shown in the table, with the increase of BCl_3, oxygen was removed by the formation of volatile BO_xCl_y in addition to the decrease of Cl on the AAO surface. Therefore, the increase of AAO etch rate with the increase of BCl_3 up to 60% in Fig. 1 is also related to the formation of BO_xCl_y and the removal of oxygen from the AAO surface. However, the decrease of AAO etch rate at the higher BCl_3 percentage shown in Fig. 1 is also related to the decrease of

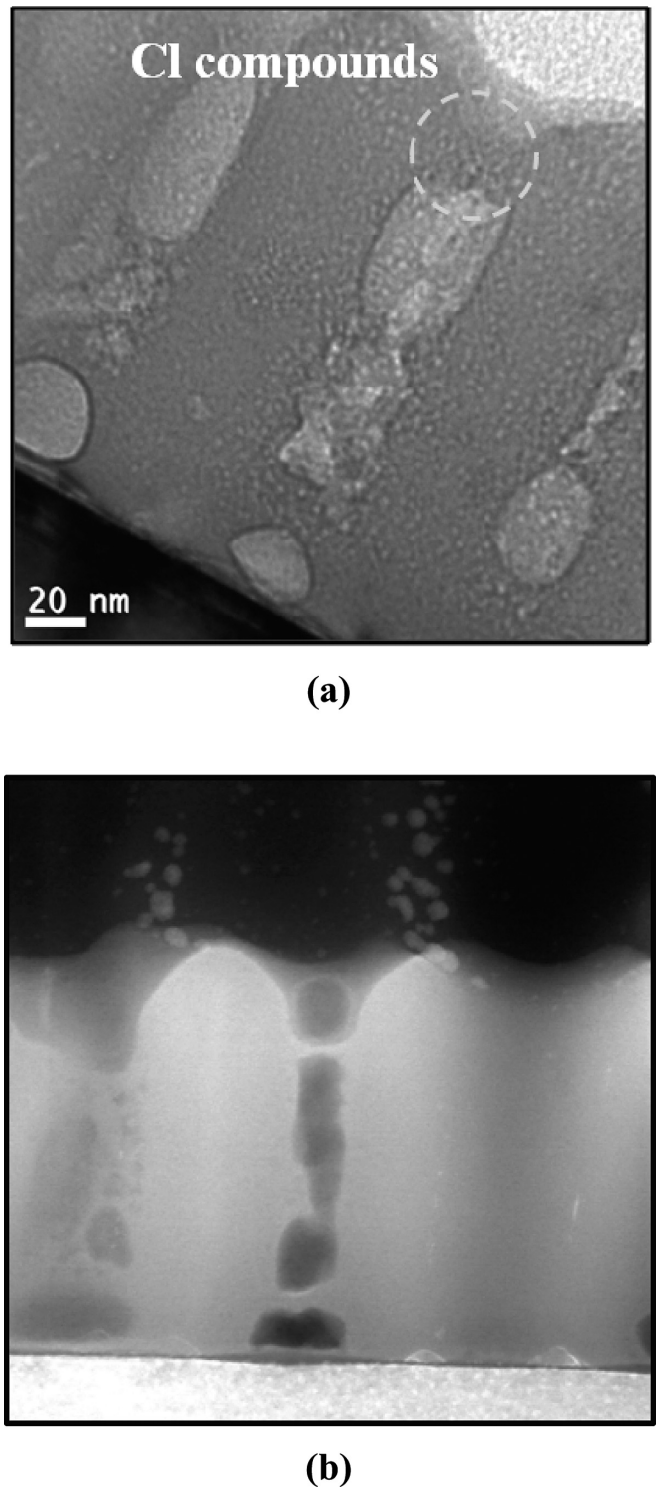

Figure 4. Cross-section TEM images of AAO on silicon after the etching with pure Cl_2 with the neutral beam shown in Fig. 3b. (a) TEM figure and (b) STEM figure showing the blocked AAO pore by the etching with pure Cl_2.

dissociated Cl on the AAO surface with the increase of BCl_3 due to the removal of Cl required for the formation of volatile $AlCl_x$ from the AAO surface by the formation of volatile byproducts such as BO_xCl_y.

Using the highest AAO etch rate condition of Cl_2(40%)/BCl_3(60%), the AAO was etched by the neutral beam and the ion beam and the FESEM micrographs of the etched AAO samples are shown in Fig. 6. The other etch conditions were the same as those

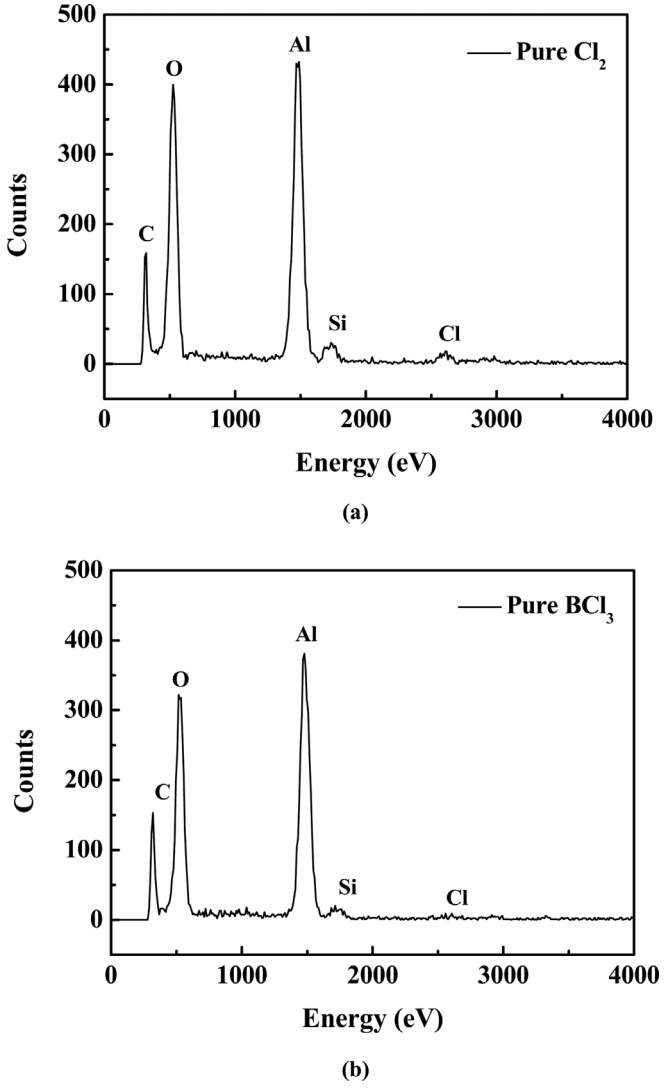

Figure 5. Micro EDX data of AAO pore sidewall etched by the neutral beam with (a) pure Cl_2 and (b) pure BCl_3 shown in Fig. 3.

shown in Fig. 1. As shown in the figure, for the AAO etched by Cl_2(40%)/BCl_3(60%) neutral beam, the barrier layer was removed, however, for the AAO etched by the Cl_2(40%)/BCl_3(60%) ion beam, the barrier layer was difficult to be etched until almost all of the AAO thickness was etched away in addition to the destruction of the AAO pore structure. In addition, for all of the Cl_2/BCl_3 gas mixture conditions, the barrier layer was not easily etched using the ion beam similar to the reactive ion etching of AAO conducted by other researchers.[22] The difficulty in the etching of the barrier layer by the conventional reactive ion etching or by the ion beam shown in Fig. 6 is believed to be related to the charging of the AAO surface by the incident ions during the etching.

Table I. Atomic composition of AAO surface before and after the etching by Cl_2/BCl_3 neutral beam for different Cl_2/BCl_3 percentages.

Cl_2/BCl_3 gas mixture	Al	O	Cl	B
Before etching	26.7	73.3	—	—
Cl_2 10 sccm	20.8	76.5	2.7	—
Cl_2 4 sccm BCl_3 6 sccm	25.6	73.2	0.9	0.4
Cl_2 2 sccm BCl_3 8 sccm	26.9	72.6	0.9	0.4
BCl_3 10 sccm	28.3	70.8	0.5	0.4

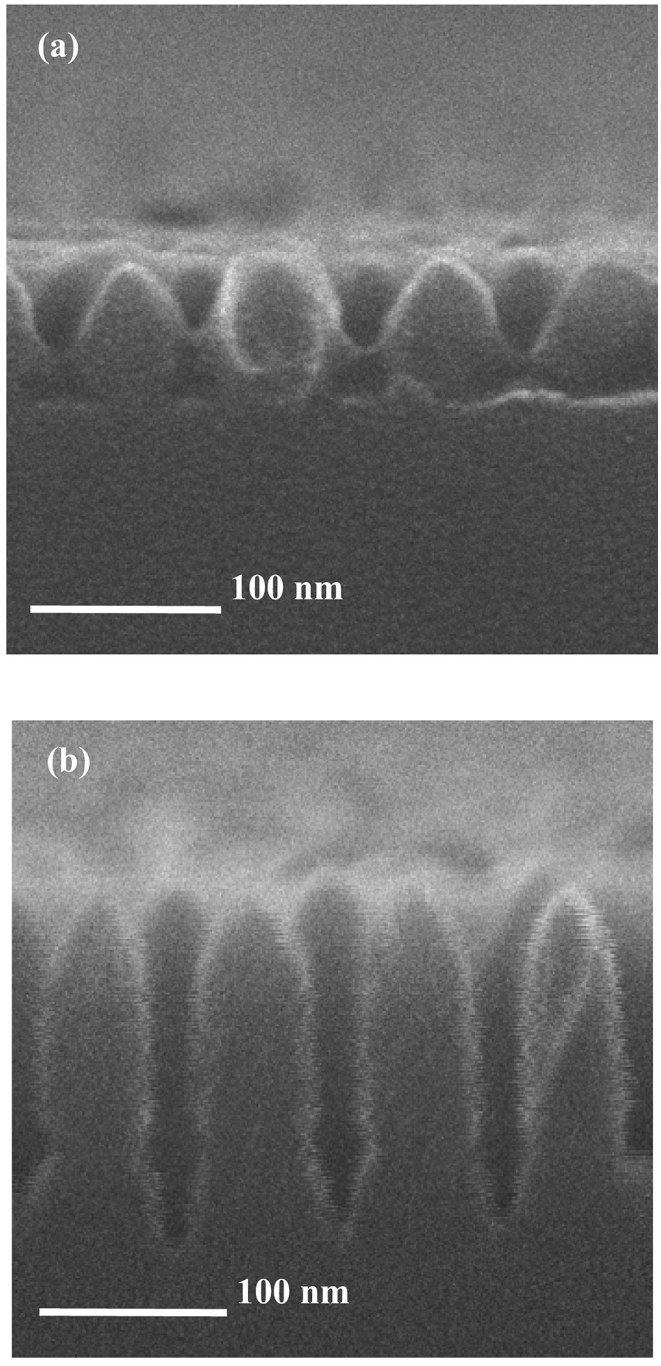

Figure 6. SEM micrographs of AAO on silicon etched with the highest AAO etch rate condition of BCl_3(60%)/Cl_2(40%) using (a) the ion beam and (b) the neutral beam.

Figure 7 shows the schematic drawing of the possible particle trajectories during the AAO etching by a neutral beam and an ion beam. During the etching by the ion beam or by the conventional reactive ions, the bottom and sidewall of AAO pore are charged positively by the incident reactive ions and, when the charging is high enough, the incident ions can not reach the bottom of AAO due to the change of ion trajectory as shown in the figure. However, in the case of neutral beam, due to the lack of charging, the incident particle can reach and bombard the bottom of the AAO. Therefore, the barrier layer located at the bottom of the AAO pore could be etched easily by the neutral beam and by using BCl_3 containing Cl_2 gas mixture for the removal of oxygen from the AAO surface for the etching.

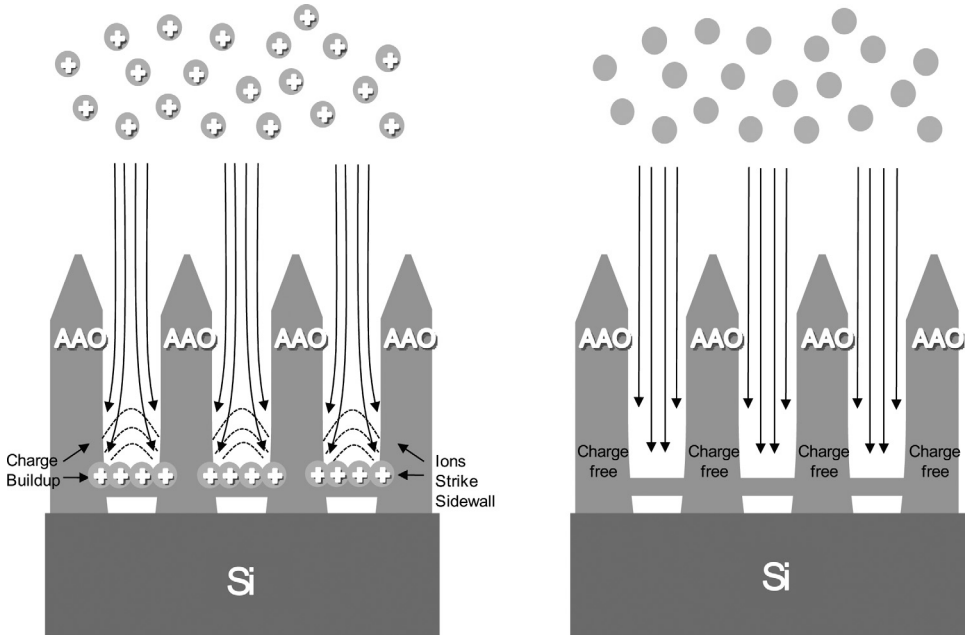

Figure 7. Schematic drawing of the possible particle trajectories during the AAO etching by a neutral beam and an ion beam.

Conclusions

The barrier layer of AAO formed on the silicon substrate was etched using a neutral beam and an ion beam in Cl_2/BCl_3 gas mixtures and their etch mechanisms were investigated. The etch rate of AAO itself was increased with the increase of BCl_3 percentage up to 60% of BCl_3, however, the further increase of BCl_3 percentage decreased the AAO etch rate for both the neutral beam and the ion beam. The etching of AAO itself was related to the Cl radical density in the plasma and the formation of volatile BO_xCl_y on the AAO surface. When the neutral beam etching was used, the barrier layer was not etched using pure Cl_2 due to the formation of less volatile $AlCl_xO_y$ on the AAO pore sidewall and by the blocking the pore during the etching. By the etching with BCl_3 containing gas mixtures, the barrier layer was successfully removed due to the formation of volatile BO_xCl_y during the etching. However, when the barrier layer was etched using the ion beam with the BCl_3 containing gas mixtures, even though AAO itself is etched, the barrier layer located near the bottom of the AAO pore was not easily etched due to the charging of the AAO pore similar to the case of conventional reactive ion etching. Through the successful etching of the barrier layer by the etching using the Cl_2/BCl_3 neutral beam, the minimum AAO pore diameter in the order of tens nm could be maintained and, which is beneficial in the formation of tens of nanometer size of nanostructures such as nanodot, nanorod, etc.

Acknowledgments

This work was supported by the National Research Foundation of Korea Grant funded by the Korean Government (MEST) (NRF-2010-M1AWA001-2010-0026248). This work was also supported in part by the World Class University program of National Research Foundation of Korea (Grant no. R32-2008-000-10124-0) and by the Ministry of Education, Science and Technology (2010-0015035).

Sungkyunkwan University assisted in meeting the publication costs of this article.

References

1. N. Y. Kwon, K. H. Kim, J. H. Heo, and I. S. Chung, *J. Vac. Sci. Technol. A*, **27**, 803 (2009).
2. X. Zhao, U. J. Lee, S. K. Seo, and K. H. Lee, *Mater. Sci. Eng. C*, **29**, 1156 (2009).
3. T. Xu, G. Zangari, and R. M. Metzger, *Nano lett.*, **2**, 37 (2002).
4. D. A. Brevnov, M. Barela, M. E. Piyasena, G. P. Lopez ,and P. B. Atanassov, *Chem. Mater.*, **16**, 682 (2004).
5. A. P. Li, F. Műller, A. Briner, K. Nielsch, and U. Gősele, *J. Appl. Phys*, **84**, 6023 (1998).
6. H. Masuda, H. Asoh, M. Watanabe, K. Nishio, M. NaKao, and T. Tamamura, *Adv. Mater*, **13**, 189 (2001).
7. J. K. Hong, K. H. Kim, J. H. Heo, and I. S. Chung, *Thin Solid Films*, **518**, 4572 (2010).
8. A. N. Belov, *Semiconductor*, **42**, 1519 (2008).
9. S. Kim, J. Lim, and J. Choi, *Polym. Sci. Technol.*, **17**, 742 (2006).
10. J. Liang, H. Chik, A. Yin, and J. Xu, *J. Appl. Phys.*, **91**, 15 (2002).
11. S. H. Park, S. B. Kim, D. J. Lee, S. J. Yun, Z. G. Khim, and K. B. Kim, *J. Electrochem. Soc.*, **156**, 181 (2009).
12. O. Rabin, P. R. Herz, Y. M. Lin, A. I. Akinwande, S. B. Cronin, and M. S. Dresselhaus, *Adv. Funct. Mater*, **13**, 631 (2003).
13. X. Zhao, S. K. Seo, U. J. Lee, and K. H. Lee, *J. Electrochem. Soc.*, **154**, C553 (2007).
14. M. Shaban, H. Hamdy, F. Shahin, J. Park, and S. W. Ryu, *J. Nanosci. Nanotechnol.*, **10**, 3380 (2010).
15. S. Shingubara, O. Okino, Y. Murakami, H. Sakaue, and T. Takahagi, *J. Vac. Sci. Technol. B*, **19**, 1901 (2001).
16. S. W. Shin, S. G. Lee, J. Lee, C. N. Whang, J. H. Lee, I. H. Choi, T. G. Kim, and J. H. Song, *Nanotechnology*, **16**, 1392 (2005).
17. D. H. Lee, B. J. Park, and G. Y. Yeom, *Jpn. J. Appl. Phys.*, **44**, L63 (2005).
18. B. J. Park, S. W. Kim, S. K. Kang, K. S. Min, S. D. Park, S. J. Kyung, H. C. Lee, J. W. Bae, J. T. Lim, D. H. Lee, et al., *J. Phys. D. Appl. Phys*, **41**, 024005 (2008).
19. T. H. Min, B. J. Park, S. K. Kang, G. H. Gweon, Y. Y. Kim, and G. Y. Yeom, *J. Phys. D. Appl. Phys*, **42**, 155204 (2009).
20. S. M. Koo, D. P. Kim, K. T. Kim, and C. I. Kim, *Mater. Sci. and Eng. B*, **118**, 201 (2005).
21. H. S. Seo, Y. G. Jung, S. W. Jee, J. M. Yang, and J. H. Lee, *Scr. Mater.*, **57**, 968 (2007).
22. J. C. Arnold and H. H. Sawin, *J. Appl.Phys*, **70**, 5314 (1991).